Journal of Steroid Biochemistry & Molecular Biology 121 (2010) 63–67

Contents lists available at ScienceDirect

Journal of Steroid Biochemistry and Molecular Biology

journal homepage: www.elsevier.com/locate/jsbmb

Interactions between 1α,25(OH)$_2$D$_3$ and residues in the ligand-binding pocket of the vitamin D receptor: A correlated fragment molecular orbital study☆

Kenji Yamagishi[a], Hiroaki Tokiwa[a,b], Makoto Makishima[c], Sachiko Yamada[a,c,d,*]

[a] Research Information Center for Extremophile, Rikkyo University, 3-34-1, Nishi-Ikebukuro, Toshima-ku, Tokyo 171-8501, Japan
[b] Department of Chemistry, Faculty of Science, Rikkyo University, 3-34-1, Nishi-Ikebukuro, Toshima-ku, Tokyo 171-8501, Japan
[c] School of Medicine, Nihon University, 30-1, Oyaguchi-kamicho, Itabashi-ku, Tokyo 101-0062, Japan
[d] Institute of Biomaterials and Bioengineering and School of Biomedical Sciences, Tokyo Medical and Dental University, 2-3-10, Kanda-Surugadai, Chiyoda-ku, Tokyo 101-0062, Japan

ARTICLE INFO

Article history:
Received 22 November 2009
Received in revised form 3 March 2010
Accepted 5 March 2010

Keywords:
Vitamin D receptor
Ligand–receptor interaction
Ab initio fragment molecular orbital calculation
van der Waals dispersion interaction energy
Alanine-scanning mutational analysis
Interfragment interaction energy analysis

ABSTRACT

To provide physicochemical insight into the role of each residue in the ligand-binding pocket (LBP) of the vitamin D receptor (VDR), we evaluated the energies of the interactions between the LBP residues and 1α,25(OH)$_2$D$_3$ by using an *ab initio* fragment molecular orbital (FMO) method at the Møller–Plesset second-order perturbation (MP2) level. This FMO-MP2 method can be used to correctly evaluate both electrostatic and van der Waals dispersion interactions, and it affords these interaction energies separately. We deduced the nature of each interaction and determined the importance of all the LBP residues involved in ligand recognition by the VDR. We previously reported the results of alanine-scanning mutational analysis (ASMA) of all 34 non-alanine residues lining the LBP of the human VDR. The theoretical results in combination with the ASMA results enabled us to assign the role of each LBP residue. We concluded that electrostatic interactions are the major determinant of the ligand-binding activity and ligand recognition specificity and that van der Waals interactions are important for protein folding and, in turn, for cofactor binding.

1. Introduction

1α,25-Dihydroxyvitamin D$_3$ [1α,25(OH)$_2$D$_3$], the active metabolite of vitamin D, regulates calcium and phosphorous homeostasis, cellular growth and differentiation, and immune system [1,2]. The biological effects of 1α,25(OH)$_2$D$_3$ are mediated by the vitamin D receptor (VDR; also referred to as NR1I1), which is a member of nuclear receptor (NR) superfamily of ligand-dependent transcription factors [3]. Binding of 1α,25(OH)$_2$D$_3$ to the VDR ligand-binding domain (LBD) initiates a series of molecular events that induce the activation or suppression of target genes of the VDR. Because of the substantial therapeutic potential, 1α,25(OH)$_2$D$_3$ and its synthetic analogs have long been used to treat disorders of calcium metabolism, including osteoporosis [4]. However, even though an enormous numbers of vitamin D analogs have been synthesized [5,6], their therapeutic applications to autoimmune diseases and malignant tumors are limited, owing to the calcemic side effects of these compounds (the only exception is the external application of vitamin D analogs to psoriasis lesions). For the development of selective VDR-targeting therapy, elucidating the molecular mechanism of ligand recognition by the VDR and subsequent functional interactions with various cofactors is important [7].

The VDR is an allosteric transcription factor, as are the other NRs. Ligand-binding triggers allosteric communication by changing the conformation of the VDR and, in turn, the properties of interfaces for transcriptional cofactors.

Although crystal structures of receptor/ligand/cofactor complexes give vital information, assigning the role and importance of each residue at these interfaces is difficult. With the goal of developing vitamin D drugs with differential action, we investigated the interactions between the residues (34 non-alanine) lining the ligand-binding pocket (LBP) and the ligands by alanine-scanning mutational analysis (ASMA) [8,9]. From ASMA studies we identified LBP residues that are important for transactivation. We also carried out fragment molecular orbital (FMO) calculations using the standard Hartree–Fock (HF) method to determine the nature of the hydrogen-bonding network between six residues and 1α,25(OH)$_2$D$_3$ and to explain the behavior of hydrophilic residues in ligand recognition [9,10]. These calculations enabled us to energetically evaluate the dominant interactions.

The FMO method is an approximate *ab initio*-based molecular orbital method for large molecules [11]. The method permits

☆ Special issue selected article from the 14th Vitamin D Workshop held at Brugge, Belgium on October 4–8, 2009.

* Corresponding author at: School of Medicine, Nihon University, 30-1, Oyaguchi-kamicho, Itabashi-ku, Tokyo 101-0062, Japan. Tel.: +81 42 664 1629; fax: +81 42 664 1629.
E-mail address: yamada.vd@image.ocn.ne.jp (S. Yamada).

0960-0760/$ – see front matter © 2010 Elsevier Ltd. All rights reserved.
doi:10.1016/j.jsbmb.2010.03.028

elucidation of the nature of interactions in protein–ligand systems [12,13]. In this paper, we used the *ab initio* correlated FMO method at the Møller–Plesset second-order perturbation (MP2) level to evaluate the interaction energies of the LBP residues and the ligand in the hVDR-LBD/1α,25(OH)$_2$D$_3$ complex. This FMO-MP2 method can correctly evaluate not only electrostatic but also van der Waals dispersion interactions. By comparing the calculated results with the ASMA results, we suggested the role of each of the 34 (non-alanine) LBP residues in ligand recognition and transactivation.

2. Methods

The three-dimensional data for the hVDR-LBD (Δ165-215)/1α,25(OH)$_2$D$_3$ complex were retrieved from the protein data bank (code: 1db1 [14]), and the structural defects of the data were amended and modified as reported previously [9,10]. In the FMO calculations, the VDR was divided into one-residue fragments, with cut-off points at Cα of each residue, and 1α,25(OH)$_2$D$_3$ was treated as a fragment. All FMO calculations were performed on a cluster computer system using the ABINIT-MP program.

3. Results and discussion

3.1. FMO calculation

We carried out *ab initio* FMO calculations at the correlated MP2/6-31G** level for the VDR/1α,25(OH)$_2$D$_3$ complex. The FMO-MP2 method can be used to correctly evaluate both electrostatic and van der Waals dispersion interactions, and it affords these interaction energies separately. The HF and MP2 correlation energies correspond to electrostatic and van der Waals dispersion interactions, respectively. We analyzed the energy of the interaction between each LBP residue and 1α,25(OH)$_2$D$_3$ by using interfragment interaction energy (IFIE) analysis based on FMO calculation. The results are illustrated on the three-dimensional structure of the VDR LBD (Fig. 1). This calculation indicated that all the LBP residues except I238 (shown in red) interacted stably with 1α,25(OH)$_2$D$_3$. This result contrasts with previous results [10], obtained by the FMO method at the standard HF level, which indicated that most of the hydrophobic resides have unstable interactions with 1α,25(OH)$_2$D$_3$. We were able to evaluate the energetic importance of all the LBP residues in ligand binding by means of the FMO-IFIE analysis.

3.2. Role of hydrophilic residues

The energies of the interaction between the hydrophilic residues and 1α,25(OH)$_2$D$_3$ are summarized in the upper panels of Fig. 2 in which the electrostatic and van der Waals energies are shown separately by dark grey and hatched columns, respectively. The ASMA results [9] are shown in the lower panels for comparison. As previously reported, FMO-HF calculation gave only the energies corresponding to the dark grey parts in the upper panels [10].

3.2.1. Hydrogen-bonding residues (Y143, S237, R274, S278, H305, and H397)

Hydrophilic residues Y143, S237, R274, S278, H305, and H397 are within 3 Å of 1α,25(OH)$_2$D$_3$ and have large interaction energies with 1α,25(OH)$_2$D$_3$ (Fig. 2). The energy values indicate that 1α,25(OH)$_2$D$_3$ is strongly anchored in the VDR LBP by means of hydrogen bonds involving these hydrophilic residues. 1α,25(OH)$_2$D$_3$ has three hydroxyl groups (1-OH, 3-OH, and 25-OH). Each of the three hydroxyl groups forms a pincer-type hydrogen bond with a pair of residues. Our previously reported FMO-HF calculation indicated that only one residue forms a strong interaction with the corresponding hydroxyl group of 1α,25(OH)$_2$D$_3$, even though two residues are located in the vicinity of each hydroxyl group. The FMO-MP2 calculation carried out in this study included the interaction energies due to van der Waals interactions (hatched column, Fig. 2), and the results indicated that the important hydrogen-bonding interactions are those between R274, Y143, and H397 and 1-OH, 3-OH, and 25-OH, respectively. This result is consistent with our previous FMO-HF results, which included only the electrostatic interactions [10].

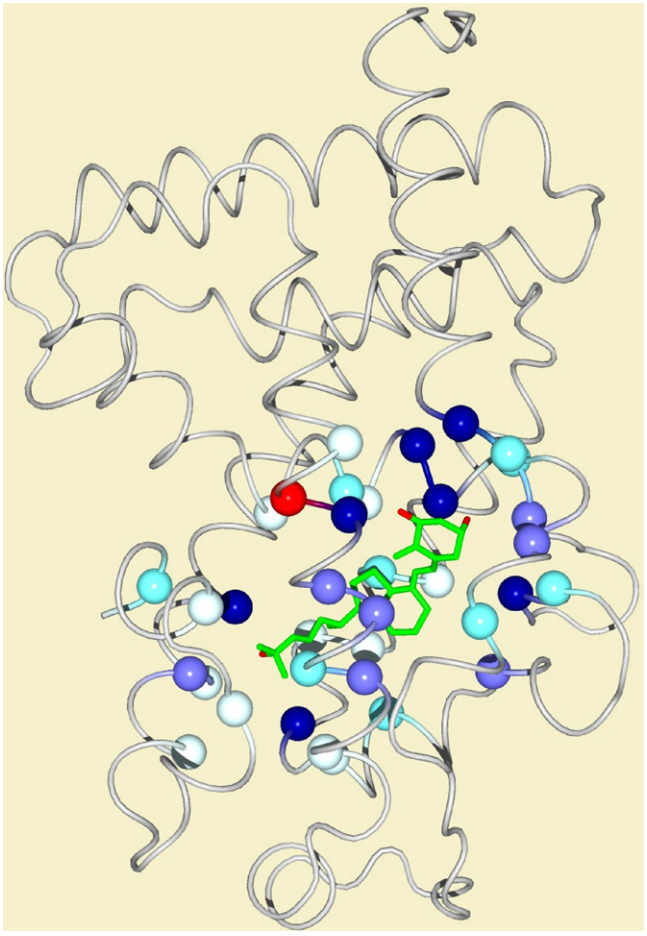

Fig. 1. Thirty six LBP residues of hVDR-LBD. The 36 LBP residues (including Ala) are shown at the Cα position with colour balls. The interaction energies of these residues with 1α,25(OH)$_2$D$_3$ calculated by the FMO-MP2 method were shown on the Cα balls by gradient colours according to the magnitude of the energy (−25.0 to −5.0 kcal/mol, dark blue; −5.0 to −2.0 kcal/mol, blue; −2.0 to −1.0 kcal/mol, cyan; −1.0 to +1.0 kcal/mol, white; +1.0 to +2.0 kcal/mol, red). The ligand 1α,25(OH)$_2$D$_3$ is shown with stick model (carbon, green; oxygen, red).

As seen in Fig. 2, the van der Waals interaction energies of these six hydrogen-bonding residues are similar; that is, the substantial differences between the overall interaction energies are due to electrostatic interactions. This finding indicates that electrostatic interactions are the key in determining the ligand specificity. The calculated interaction energies are consistent with ASMA results [9]: the larger the interaction energy, the bigger the potency-reducing effect of the mutation.

3.2.2. Other hydrophilic residues (D144, Y147, K240, S275, E277, S295, Q400, and Y401)

The interaction energies of other hydrophilic residues are also shown in Fig. 2. For these residues, the interaction energies and the ASMA result are not well correlated. For example, like the hydrogen-bonding residues, S275 interacts strongly

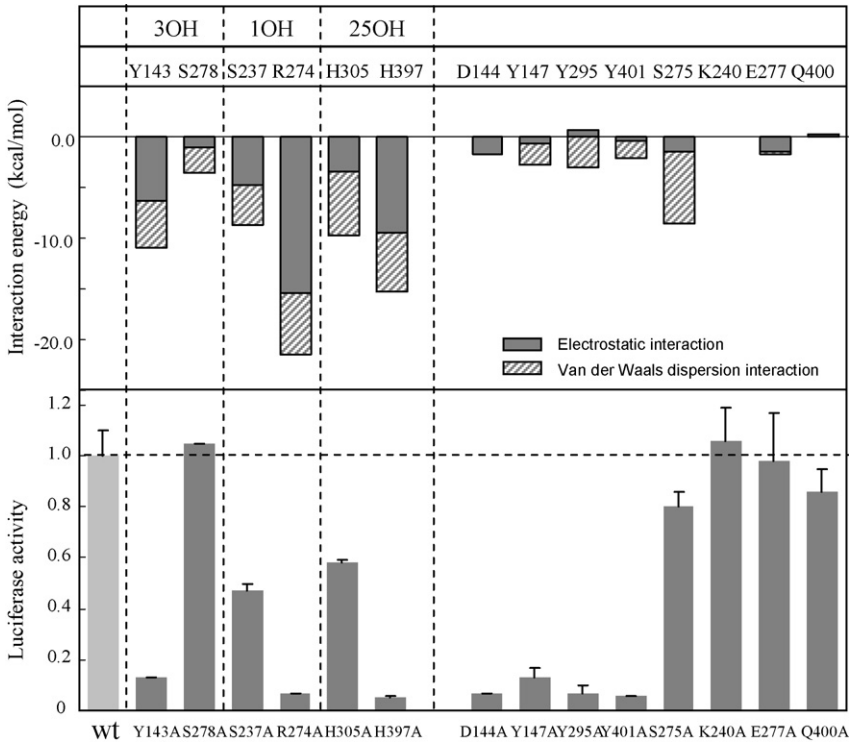

Fig. 2. Energies of interactions between hydrophilic residues and 1α,25(OH)$_2$D$_3$ in comparison with ASMA results. The interaction energies calculated by the FMO-MP method are shown in the upper panels. The electrostatic (dark grey) and van der Waals (hatched) interaction energies are shown separately. In the lower panels, the transcriptional activities of VDR one-point mutants (ASMA results) relative to that of the wild-type VDR (normalized to 1) are shown.

with 1α,25(OH)$_2$D$_3$, but S275A mutation shows little effect on transactivation. The interaction energy with the ligand is large (−8.53 kcal/mol), and the van der Waals term (−7.05 kcal/mol) is predominant. S275 has close hydrophobic interactions with the 5,7-diene via the CβH$_2$ group, and these interactions are not markedly affected by mutation to alanine. Also a serine-to-alanine mutation has only a minor effect on the stereochemical feature of the residue. These facts explain why S275A mutation has little effect on the transactivation potency, in spite of the importance of S275 inferred from its interaction energy.

Y147, Y295, and Y401 are essential for transactivation, as indicated by the ASMA results. Y147 and Y295 have close contact with 1α,25(OH)$_2$D$_3$ (they are 3–4 Å away from it), have moderate interaction energies, and may also play a role in folding the β-turn side. Y401 (4–5 Å) is at the C-terminal part of H11, which has some interaction with the ligand, and can be expected to play a key role in folding the active conformation of the VDR LBD and the coactivator interface. The marked changes in the bulkiness and shape that result from this type of mutation (tyrosine to alanine) are an additional reason for the substantial reduction in transactivation activity. D144, K240, E277, and Q400 barely interact with the ligand; they are more than 5 Å away from it. Of these four residues, only D144 is essential, because it is involved in a hydrogen-bonding network inside the water channel at the β-turn side of the LBP and plays an important role in folding.

3.3. Role of hydrophobic residues

The interaction energies of the hydrophobic LBP residues with 1α,25(OH)$_2$D$_3$ are shown in the upper panel of Fig. 3. The interactions are mostly van der Waals dispersion interactions. The ASMA results for these residues [9] are also shown (lower panel). The interaction energies for the hydrophobic residues do not correlate to the ASMA results, even for the same kinds of amino acids located similar distances from 1α,25(OH)$_2$D$_3$ (Fig. 3). The reason for this result is that the van der Waals interactions are not unidirectional but are formed evenly all around; these residues generally interact not only with the ligand but also with nearby residues that are involved in protein folding.

3.3.1. Leucine residues (L227, L230, L233, L309, L313, L404, and L414)

L227, L230, and L233 are within 4 Å of 1α,25(OH)$_2$D$_3$ and are essential residues, as indicated by ASMA [8,9], but the interaction energies of these residues differ substantially. L233 interacts only with the ligand; its interaction energy with the ligand is significantly larger than the interaction energies of the others. In contrast, L227 and L230 interact not only with the ligand but also with residues in other units of the secondary structure. These residue–residue interactions may be important for folding of the cofactor interfaces. L309, L404, and L414 have similar interaction energies with 1α,25(OH)$_2$D$_3$, as indicated by IFIE analysis, and have similar importance for transactivation, as shown by ASMA [8,9,15]. L309 (loop 6–7) interacts with the residues on H10/11; therefore, this residue may be important for the folding of the dimer interface. L404 (H11) interacts with the residues on loop 11–12, loop 6–7, and H3 and may be important for AF2 folding. L414 (loop 11–12) may be important for AF2 folding which interacts with the residues on H11 and H3. L313 (H7), which shows a moderately strong interaction with the ligand, is not very important for transactivation as shown by ASMA.

3.3.2. Isoleucine residues (I238, I268, I271, I310, and I314)

I271 is located 3–4 Å away from the ligand and is essential for transactivation; its interaction energy with the ligand is larger than the energies for the other isoleucine residues. Located on H4/5, it interacts with the residues on H3 (I238, S237, and V234) and may play key roles in the packing of H3 and H4. I268 (H4/5) is moder-

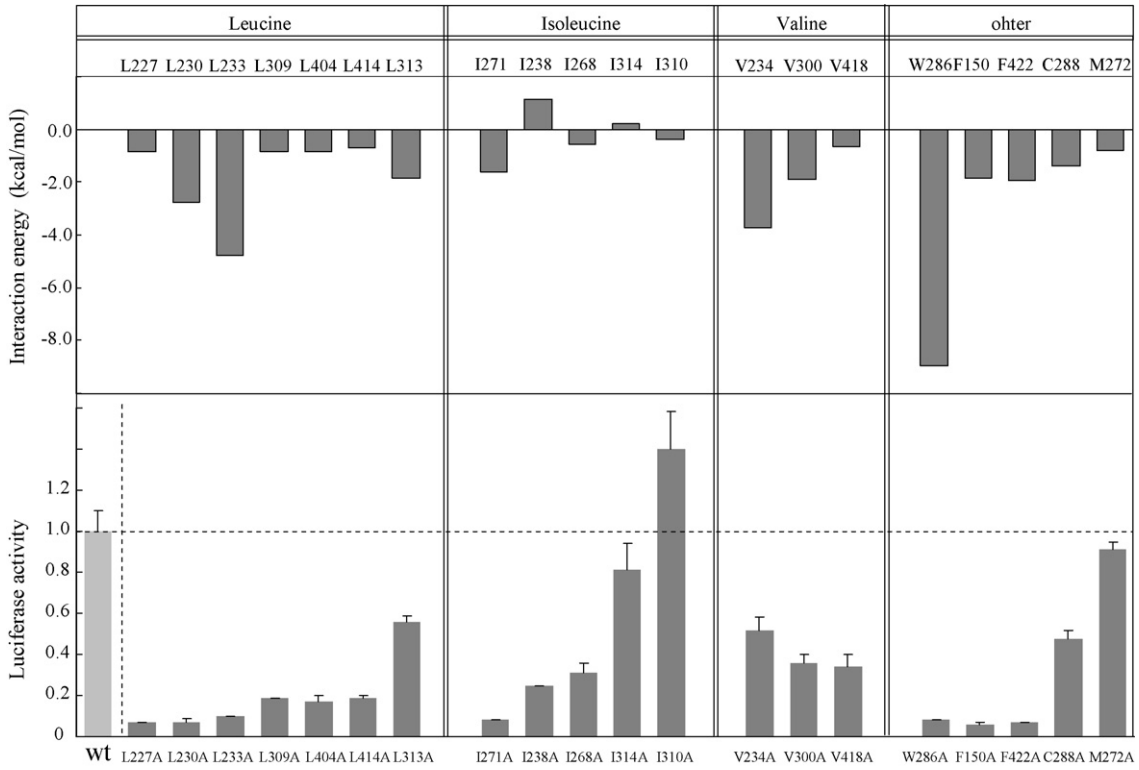

Fig. 3. Energies of interactions between hydrophobic LBP residues and 1α,25(OH)$_2$D$_3$ in comparison with ASMA results. The energies calculated by the FMO-MP2 method (upper panels) are compared with the ASMA results (lower panels).

ately important for transactivation but interacts only weakly with the ligand. It interacts with the residues on H11 and H12 and plays an important role in AF2 folding. I238 (H3) which is more than 5 Å away from the ligand, has a repulsive interaction with the ligand. However, I238 interacts with I271 (H4) and L417 (H12), connecting H3 to H4 and H12 and thus playing a key role in forming the coactivator interface. I310 and I314 are not important for transactivation and play a small role in both ligand binding and protein folding.

3.3.3. Valine residues (V234, V300, and V418)

Three valine residues (V234, V300, and V418) are located 3–4 Å from 1α,25(OH)$_2$D$_3$, but the energies of the interactions with 1α,25(OH)$_2$D$_3$ differ substantially (Fig. 3). Interestingly the interaction energies and the ASMA results are inversely correlated. V418 is moderately important for transactivation, even though its interaction energy with 1α,25(OH)$_2$D$_3$ is rather low. V418 is located on H12 and plays a role in forming the coactivator interface and the active conformation.

3.3.4. Other hydrophobic residues (F150, M272, W286, C288, and F422)

The ASMA study indicated that W286, F150, and F422 are essential for transactivation (Fig. 3) [9], but their interaction energies differ substantially. In particular, the importance of W286 (3–4 Å from the ligand) is indicated by the large van der Waals dispersion interaction with 1α,25(OH)$_2$D$_3$ (−8.73 kcal/mol); this value is larger than the values for all the other residues in the LBP. In contrast, the electrostatic interaction is small (−0.30 kcal/mol). The large van der Waals interaction energy is caused by the intense (proton-π) interactions between the indole ring of the tryptophan and the C/D ring and the 5,7-diene moiety of 1α,25(OH)$_2$D$_3$ (Fig. 3). The missense mutation W286R in the VDR is known to cause severe vitamin D-resistant rickets. The loss of the large van der Waals interaction between W286 and 1α,25(OH)$_2$D$_3$ is a cause for this condition. Our calculated interaction energies show that F150 and F422 make moderately contact with 1α,25(OH)$_2$D$_3$. In contrast, M272 and C288 have small interaction energies with 1α,25(OH)$_2$D$_3$.

4. Conclusion

We performed all-electron FMO calculations of the hVDR-LBD/1α,25(OH)$_2$D$_3$ complex at the correlated MP2/6-31G** level and evaluated the energies of the interactions between the LBP residues and 1α,25(OH)$_2$D$_3$ by using FMO-IFIE analysis. We were able to evaluate electrostatic and van der Waals dispersion interaction energies separately and explicitly. As a result, we were able to deduce the nature of each interaction and assign the importance of all the LBP residues in ligand recognition by the VDR. The FMO results in combination with ASMA results allowed us to suggest which residues play a role in protein folding. This method can be easily extended to the analysis of residue–residue interaction in protein/protein complexes, such as VDR–coactivator and VDR–retinoid X receptor (RXR) complexes and would afford invaluable information for elucidating the mechanism of allosteric communication.

Acknowledgement

This work was supported by Frontier Project “Adaptation and Evolution of Extremophile” from the Ministry of Education, Culture, Sports, and Technology of Japan.

References

[1] R. Bouillon, W.H. Okamura, A.W. Norman, Structure–function relationship in the vitamin D endocrine system, Endocr. Rev. 16 (1995) 200–257.
[2] H.F. Deluca, Evolution of our understanding of vitamin D, Nutr. Rev. 66 (2008) S73–87.

[3] D.J. Mangelsdorf, C. Thummel, M. Beato, P. Herrlich, G. Schutz, K. Umesono, B. Blumberg, P. Kastner, M. Mark, P. Chambon, R.M. Evans, The nuclear receptor superfamily: the second decade, Cell 83 (1995) 835–839.
[4] M.J. Beckman, H.F. Deluca, Modern view of vitamin D_3 and its medicinal uses, Prog. Med. Chem. 35 (1998) 1–56.
[5] H.F. DeLuca, L.A. Plum, M. Clagett-Dame, Selective analogs of 1α,25-dihydroxyvitamin D_3 for the study of specific functions of vitamin D, J. Ster. Biochem. Mol. Biol. 103 (2007) 263–268.
[6] M. Nakabayashi, S. Yamada, N. Yoshimoto, T. Tanaka, M. Igarashi, T. Ikura, N. Ito, M. Makishima, H. Tokiwa, H.F. DeLuca, M. Shimizu, Crystal structures of rat vitamin D receptor bound to adamantyl vitamin D analogs: structural basis for vitamin D receptor antagonism and partial agonism, J. Med. Chem. 51 (2008) 5320–5329.
[7] S. Yamada, M. Shimizu, K. Yamamoto, Structure–function relationships of vitamin D including ligand recognition by the vitamin D receptor, Med. Res. Rev. 23 (2003) 89–115.
[8] M. Choi, K. Yamamoto, T. Itoh, M. Makishima, D.J. Mangelsdorf, D. Moras, H.F. DeLuca, S. Yamada, Interaction between vitamin D receptor and vitamin D ligands: two-dimensional alanine scanning mutational analysis, Chem. Biol. 10 (2003) 261–270.
[9] K. Yamamoto, D. Abe, N. Yoshimoto, M. Choi, K. Yamagishi, H. Tokiwa, M. Shimizu, M. Makishima, S. Yamada, Vitamin D receptor: ligand recognition and allosteric network, J. Med. Chem. 49 (2006) 1313–1324.
[10] K. Yamagishi, K. Yamamoto, S. Yamada, H. Tokiwa, Functions of key residues in the ligand-binding pocket of vitamin D receptor: fragment molecular orbital–interfragment interaction energy analysis, Chem. Phys. Lett. 420 (2006) 465–468.
[11] K. Kitaura, T. Sawai, T. Asada, T. Nakano, M. Uebayasi, Pair interaction molecular orbital method: an approximate computational method for molecular interactions, Chem. Phys. Lett. 312 (1999) 319–324.
[12] T. Harada, K. Yamaigishi, T. Nakano, K. Kitaura, H. Tokiwa, Ab initio fragment molecular orbital study of ligand binding to human progesterone receptor ligand-binding domain, Naunyn-Schmiedeberg's Arch. Pharmacol. 377 (2008) 607–615.
[13] T. Yoshida, K. Yamagishi, H. Chuman, QSAR Study of cyclic urea type HIV-1 PR inhibitors using ab initio MO calculation of their complex structures with HIV-1 PR, QSAR Comb. Sci. 27 (2008) 694–703.
[14] N. Rochel, J.M. Wurtz, A. Mitschler, B. Klaholz, D. Moras, The crystal structure of the nuclear receptor for vitamin D bound to its natural ligand, Mol. Cell 5 (2000) 173–179.
[15] M.T. Mizwicki, C.M. Bula, P. Mahinthichaichan, H.L. Henry, S. Ishizuka, A.W. Norman, On the mechanism underlying (23*S*)-25-dehydro-1α(OH)-vitamin D_3-26,23-lactone antagonism of hVDRwt gene activation and its switch to a superagonist, J. Biol. Chem. 284 (2009) 36292–36301.